Applied Energy 94 (2012) 244–250

Contents lists available at SciVerse ScienceDirect

Applied Energy

journal homepage: www.elsevier.com/locate/apenergy

A dynamic model based on the piston flow concept for the thermal characterization of solar collectors

N. Amrizal [a,b], D. Chemisana [b,*], J.I. Rosell [b], J. Barrau [b]

[a] University of Lampung, J/Sumantri.B 1, 35145 Bandar Lampung, Indonesia
[b] University of Lleida, c/Pere de Cabrera s/n, 25001 Lleida, Spain

ARTICLE INFO

Article history:
Received 14 November 2011
Received in revised form 24 January 2012
Accepted 30 January 2012

Keywords:
Solar thermal collector
Piston flow concept
Thermal characterization
Transient model
Dynamic testing experiments

ABSTRACT

A simple, transient model for the characterization of the dynamic thermal performance of solar thermal collectors was developed and experimentally validated. The proposed model equation is linear with respect to the input parameters and does not require any treatment for ordinary differential equations (ODEs). The temperature distribution in the fluid flowing inside the collector is described by means of the piston flow and finite increment concepts. The dynamic effect, for a given flow rate, is expressed by the heat transport time and is based on the effective thermal capacity of the collector. The results reveal that the characteristic parameters involved in the model agree reasonably well with the experimental variables obtained from standard steady-state measurements. After a calibration process the model can well predict the thermal performance of a solar thermal collector, for a specific weather data set.

1. Introduction

Solar collectors thermal performance can be characterized by a steady-state or a dynamic model. Research concerning dynamic modelling is essential to adequately characterize the transient behavior of solar thermal collectors. At this point it should be mentioned that a dynamic model can be very useful because it provides information about the collector behavior and facilitates experimental tests in comparison with the steady-state and the quasi-dynamic standard tests. In the literature there are several studies about these types of models, however only a few of them regard the dynamic performance of solar thermal collectors.

In terms of the steady-state testing, the EN 12975 standard, the ISO 9806-1 and the ANSI/ASHRAE 93-2003 are available for characterizing and rating a collector under outdoor testing conditions [1–3]. These standards have been adopted worldwide as reference methodologies for solar thermal collectors testing. Nevertheless, steady-state outdoor testing includes several difficulties associated with the weather conditions. In many places in the world and over many periods through the year, the weather conditions do not fulfil the requirements for the steady-state testing standards defined in EN 12975 [2].

Thus, in order to overcome the difficulties associated with the steady-state testing, transient testing methods have been developed and reported in the literature [1,4–8]. The EN 12975 standard includes a procedure for partially transient testing. This standard is based on the so called one-node, one-segment model [4] and takes into account effects such as the second-order processes, wind speed and long-wave irradiance dependence of heat losses. However, there are restrictive requirements associated with the constant inlet fluid temperature and predominant weather conditions; experimental testing difficulties arise from both. Furthermore, it is essential to have large enough variability of solar radiation during the test in order to increase the thermal capacitance effects. In addition, if some conditions are not fulfilled during the testing period, then an extra testing day is required.

On the other hand, Muschaweck and Spirkl [6] proposed a dynamic solar collector (DSC) performance testing and developed the model and the computation procedure. The model is an extension of the Hottel-Whillier-Bliss equation to a dynamic model with simple collector parameters: zero loss efficiency, slope of the characteristic curve and thermal mass. The collector is considered as split into *N*-segments connected in series and by connecting them the overall behavior is then determined. The method allows arbitrary variations of irradiance, ambient temperature, inlet temperature and fluid flow rate during the test. Although the model should be simple and practical for rating the collector under outdoor conditions, the authors reported that there are difficulties in determining the heat thermal capacity parameter. This is presumably because results are obtained from a large time step in the experimental data (5 min) and from the crude way of modelling the collector thermal capacity. Moreover, the method requires the use of a specific ODE solver such as Lavenberg-Marquardt.

* Corresponding author. Tel.: +34 973003711; fax: +34 973003575.
E-mail address: daniel.chemisana@macs.udl.cat (D. Chemisana).

0306-2619/$ - see front matter © 2012 Elsevier Ltd. All rights reserved.
doi:10.1016/j.apenergy.2012.01.071

Nomenclature

A_c	absorber plate area of the collector (m^2)
A_s	absorber plate area of the collector segment (m^2)
c_f	specific heat capacity of the fluid (J/kg K)
c_1, c_2, c_3	model parameters: c_1 (Km^2/W), c_2 and c_3 (–)
F'	collector efficiency factor (–)
G	solar radiation (W/m^2)
K_θ (θ)	incidence angle modifier (–)
$\dot{m}_f$	mass flow rate of the fluid (kg/s)
$m_e c_e$	effective thermal capacity of a segment (J/K)
$M_e c_e$	effective thermal capacity of the collector (J/K)
nt	number of time steps
N	number of segments
t	time (s)
T	outlet temperature (K)
T_a	ambient temperature (K)
T_0	inlet temperature (K)
T_{ix}^{it}	fluid temperature at segment *ix* and time interval *it* (K)
U_L	overall convective heat loss coefficient of the collector ($W/(m^2K)$)
U_1	convective heat loss coefficient at $(T_m - T_a) = 0$ ($W/(m^2K)$)
U_2	wind-induced convective heat loss coefficient ($J/(m^3K)$)
Greek symbols	
Δt	time step, time interval (s)
θ	incidence angle (°)
v	wind velocity (m/s)
$(\tau\alpha)_{en}$	normal incidence transmittance-absorbance product (–)
τ_c	collector time constant (s)
τ_t	heat transport time (s)

Nayak et al. [7] studied three transient methods for testing solar flat-plate thermal collectors: Perers, DSC and Wijeysundera. The main conclusions revealed are: Perers method generates simulated results close to the steady state value (within 4%), whereas DSC and Wijeysundera methods underpredict it (maximum deviation ≈ 10%). In addition, DSC model shows large variation in the values of the heat thermal capacity parameter. Test set-up and procedures for both Perers and DSC methods are simpler in comparison to Wijeysundera method. Perers method requires control of the inlet fluid temperature while DSC method does not require flow rate and fluid inlet temperature control.

A comparison between stationary and dynamic solar collector models in terms of the energy yield, including DSC model, was conducted by Scnieders [8]. According to this study, 2-nodes model did show the best description of the actual collector behavior. Within 1-node methodologies, DSC model did show a better parameter identification of the collector than MFC (Matched Flow Collector) [5] and even better than 2-nodes model.

A dynamical simulation of a thermosyphonic flat-plate collector, using 3-nodes and 1-segment models, was developed and experimentally validated by Taherian et al. [9]. The governing differential equations were separately written for the absorber, the glass cover and the working fluid, and then solved as a system of equations. This model was capable of predicting system efficiency during sunny days, but on partially cloudy days, it only gave proper results for the glass cover temperature; however, it accurately predicted the mean collector fluid temperature. The authors attributed this behavior to the difference in the simulation time-step resolution and that of the climate data imported into the program.

In the present work, a dynamic model based on the piston flow concept was developed. This concept simplifies DSC model in terms of building an algebraic expression for describing the distribution of fluid temperature through the collector. The purpose of this simplification is to obtain a model that can be handled more easily with any spreadsheet programs using simple expressions. Furthermore, the method allows arbitrary variations of irradiance, ambient temperature and inlet temperature during the test. At this point it should be mentioned that the model has been validated in a Photovoltaic/Thermal (PV/T) flat-plate solar collector (Fig. 1a); however it can be applied to different collectors within the same range of the effective thermal capacity per collector aperture unit area. Although the model covers only the collectors which behave according the piston flow concept conditions, most of the commercial solar thermal collectors fulfils these requirements. The results revealed that the proposed model did show a good behavior, therefore can be used for the thermal performance characterization of solar thermal collectors.

2. The mathematical model

The dynamic model used in the present study is a simplification of the DSC model proposed by [6]. At the same time, the proposed model is an approximation of a Partial Differential Equation (PDE) which governs collector behavior by an Ordinary Differential Equation system (ODEs). In the DSC model the collector is divided into N equal parts and each segment is modelled by one ODE as given by:

$$(m_e c_e)\frac{dT}{dt} = A_s[F'(\tau\alpha)_{en}K_\theta(\theta)G - F'U_L(T - T_a)] - \dot{m}_f c_f(T - T_0) \quad (1)$$

where $(m_e c_e)$ is the effective thermal capacity of the segment, $\dot{m}_f$ is the mass flow rate of the fluid, c_f is the specific heat capacity of the fluid, $F'(\tau\alpha)_{en}$ is the zero loss efficiency for global radiation at normal incidence, G is the solar radiation, F' is the collector absorber efficiency factor, U_L is the overall heat loss coefficient, T and T_0 are the fluid temperatures of the segment and at its entrance, T_a is the ambient temperature, A_s is the absorber plate area of the collector segment and $K_\theta(\theta)$ is the incident angle modifier.

In order to derive from Eq. (1) a simple algebraic expression, the piston flow concept is adopted. This concept is based on the fact that the fluid which enters in the first element displaces the fluid of the second element and so on. For the model development, the following assumptions have been adopted:

1. The fluid temperatures are considered to be constant at each segment.
2. Heat transfer processes are considered to be one dimensional.
3. The mass flow rate is considered constant in time.
4. The specific heat of the fluid and the overall heat loss coefficient are assumed to be constant with temperature.

DSC model equation can be simplified considering the outlet fluid temperature of the previous segment at the previous time interval, as the inlet fluid temperature. The derivative term is approximated through finite increments and the drag term is explicitly approached, considering the previous time step values. Thus, Eq. (1) can be expressed by:

$$(m_e c_e)\frac{(T_{ix}^{it} - T_{ix}^{it-1})}{\Delta t} = A_s\left[F'(\tau\alpha)_{en}K_\theta(\theta)G^{it} - F'U_L(T_{ix}^{it} - T_a^{it})\right] - \dot{m}_f c_f\left(T_{ix}^{it-1} - T_{ix-1}^{it-1}\right) \quad (2)$$

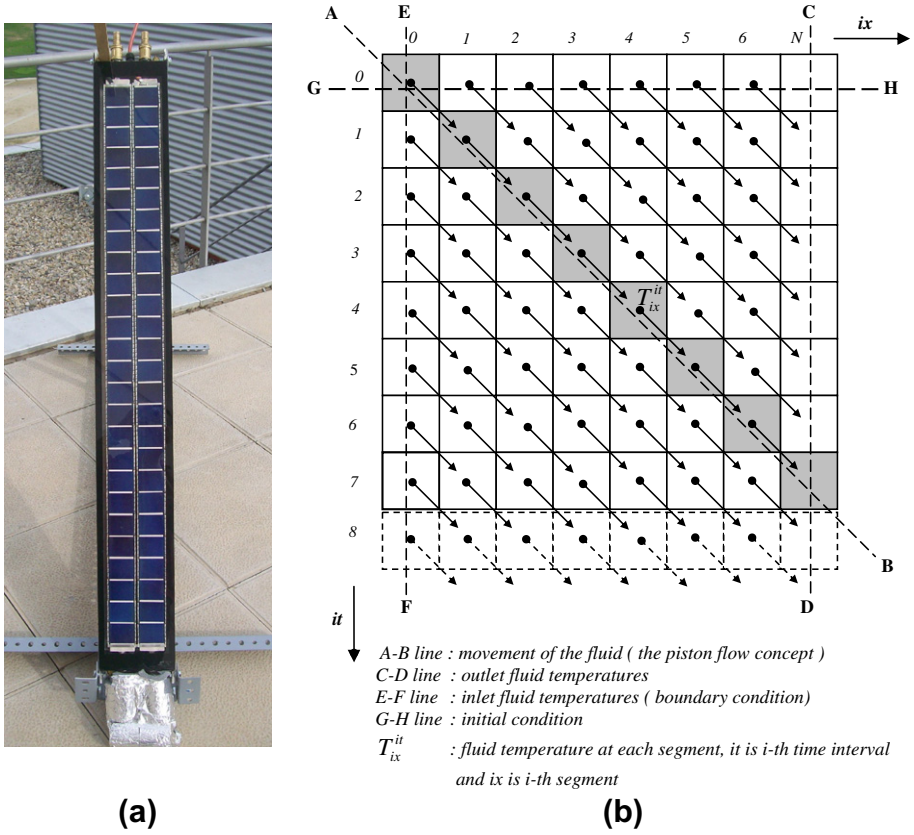

Fig. 1. (a) Picture of the PV/T collector; (b) a schematic diagram of the fluid movement through the collector according to the piston flow concept.

where the T_{ix}^{it-1} is the fluid temperature at the previous time interval and T_{ix-1}^{it-1} is the fluid temperature at the previous segment as well as at the previous time interval. In Fig. 1b schematic diagram of the fluid movement through the collector according to the piston flow concept is illustrated.An additional approach to simplify the model described in Eq. (2) is applied if the time interval Δt, associated with the sampling rate selected, fulfils the following equation:

$$\frac{m_e c_e}{\Delta t} = \dot{m}_f c_f \tag{3}$$

Then, Eq. (2) may be rewritten as:

$$\dot{m}_f c_f (T_{ix}^{it} - T_{ix-1}^{it-1}) = A_s[F'(\tau\alpha)_{en} K_\theta(\theta) G^{it} - F' U_L (T_{ix}^{it} - T_a^{it})] \tag{4}$$

and re-arranging Eq. (4) leads to:

$$T_{ix}^{it} = \frac{F'(\tau\alpha)_{en} K_\theta(\theta) G^{it} A_s + F' U_L T_a^{it} A_s + \dot{m}_f c_f T_{ix-1}^{it-1}}{\dot{m}_f c_f + F' U_L A_s} \tag{5}$$

Eq. (5) can be written in a more compact form by defining some coefficients. In this way, only temperature and irradiance variables appear directly in the equation:

$$T_{ix}^{it} = c_1 G^{it} + c_2 T_a^{it} + c_3 T_{ix-1}^{it-1} \tag{6}$$

where $c_1 = \frac{F'(\tau\alpha)_{en} K_\theta(\theta) A_s}{\dot{m}_f c_f + F' U_L A_s}$, $c_2 = \frac{F' U_L A_s}{\dot{m}_f c_f + F' U_L A_s}$ and $c_3 = \frac{\dot{m}_f c_f}{\dot{m}_f c_f + F' U_L A_s}$

In the majority of conventional flat-plate solar thermal collectors, the term $\dot{m}_f c_f$ is very large compared to $F' U_L A_s$, $\dot{m}_f c_f \gg F' U_L A_s$, therefore it can be considered that the coefficient c_3 is equal to 1.

Finally, Eq. (6) is expressed temporally and spatially in order to obtain a simple algebraic equation as a function of the external G, T_a and T_0:

$$T_{ix}^{it} = c_1 \sum_{i=0}^{i=ix-1} G^{it-i} + c_2 \sum_{i=0}^{i=ix-1} T_a^{it-i} + T_0^{it-ix} \tag{7}$$

where it and ix refer to the ith interval time and ith segment along the collector tube, respectively; T_0 is the inlet temperature of the working fluid considered as a boundary condition. Eq. (7) is within the valid range of values: $1 < ix \leqslant N$ and $ix < it \leqslant nt$; where N is the collector segments number and the nt is the total number of temporal data. When $it < ix$, Eq. (6) must be used in order to consider initial temperatures of each segment.

The dependence of U_L on wind velocity is given by the following equation:

$$U_L = U_1 + U_2 v \tag{8}$$

where U_1 is the heat loss coefficient at $(T - T_a) = 0$, v is the wind velocity and U_2 is the heat loss coefficient due to wind speed. Wind velocity variations make necessary to modify U_L and thus coefficients c_1 and c_2. In case of variable wind velocities, those coefficients must be considered as variable in each time interval. Furthermore, in agreement with the EN 12975, wind velocity can be considered to be constant if the maximum range of variation with respect to the average during the test is lower ±0.5 m/s. In terms of the present work, Eq. (7) can be considered for constant wind velocity since the wind speed was not so high in the place where experiments were conducted and the measurements were short-term.

The number of segments N can be determined by the relationship between the collector heat transport time and the interval time. The heat transport time (τ_t) is defined as the time which is needed for the flowing fluid to remove the heat stored by the solar collector.

$$\tau_t = \frac{M_e c_e}{\dot{m}_f c_f} \tag{9}$$

The effective mass in each of the collector segments is considered to be uniform over the area of the collector,

$$m_e c_e = \frac{M_e c_e}{N} \tag{10}$$

Substituting Eqs. (10) into (3), the following equation is obtained:

$$\frac{M_e c_e}{N\Delta t} = \dot{m}_f c_f \tag{11}$$

The algebraic equation, Eq. (7), should be applied with the appropriate number of segments N. This can be directly calculated from Eqs. (9) and (11) as follows:

$$N = \frac{M_e c_e}{\dot{m}_f c_f \Delta t} = \frac{\tau_t}{\Delta t} \tag{12}$$

In Fig. 2, the behavior of the experimental device and the results obtained from the model, are illustrated. It can be noticed that the results of the experimental behavior have an exponential trend while the modelled ones have a linear tendency. The main characteristics of the collector are described in Table 1. As the model is not an exponential function, the difference in temperature between the two curves at the edge point gives the maximum error. Therefore, if necessary to minimize the simulated data error this difference should be reduced. This could be achieved by setting the same time constant for both the experimental and the modelled systems by applying the following expression:

$$\tau_t = (1 - e^{-1})^{-1}\tau_c \tag{13}$$

where τ_c is the collector time constant which is defined as the elapsed time between unshielding the collector to the sun and the point where the collector outlet temperature increases to $1 - e^{-1}$ (63.2%) from the initial value.

The condition fulfilled in Eq. (13) is that the model best reproduces the exponential experimental behavior when the modelled curve is tangent to the experimental one at τ_c, as can be seen in Fig. 2. In general, experimental and modelled results show a good agreement. The maximum divergence is presented by the point 3 of Fig. 2. Based on Eqs. (12) and (13), the number of segments can be calculated by:

$$\Delta t = \frac{\tau_t}{N} = \frac{(1 - e^{-1})^{-1}\tau_c}{N} \tag{14}$$

Table 1
Data specification of the collectors.

Variables	Values
Mass flow rate (g/s)	3.17
Collector gross area (m^2)	0.146
Volume (l)	0.070
Time constant (s)	90.2
Heat transport time (s)	142.7

The benefit of using Eq. (14) is the fact that the number of segments depends directly on τ_c, which is easily determined from the experimental system. The higher the N, the higher the accuracy in the system description. In order to achieve high resolution (Eq. (14)), the interval time must be very small, arising problems associated with the processing time, the store memory, etc. A minimum value of N to describe adequately in detail the system has proved to be at least equal to or higher than 10. This means that the interval time Δt should be at least one order of magnitude (10 times) lower than τ_t. This condition is essential to obtain a proper modelled behavior.

3. Experiments

Experiments were conducted in order to collect data for the dynamic characterization of the collector based on the proposed model (Section 2). The collector was studied involving three measurement data sets regarding the steady-state characterization, the dynamic calibration of the collector and the model validation tests. The steady-state test was employed as a reference to compare the results obtained by the dynamic modelling performed. The validation process is important to confirm model accuracy. More details about the validation of the model are given in Section 4.2 while the individual test procedures are explained in the following paragraphs.

3.1. Time constant measurement

The measuring of the time constant is also required in the characterization process. As described previously, the time constant

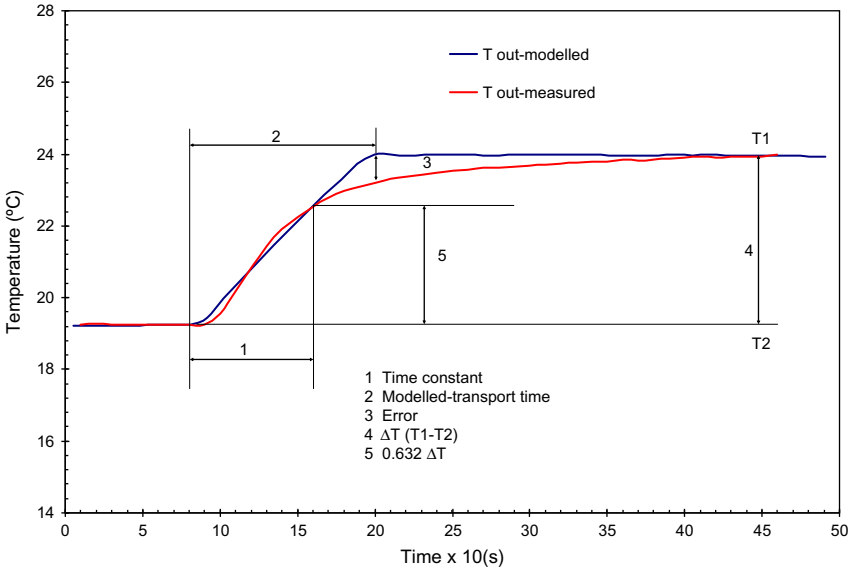

Fig. 2. Experimental and the corresponding simulated approach for time variations in the outlet temperature.

determines the time required for the outlet fluid temperature to attain 63.2% of its steady-state value following a step change in the input (Fig. 2). The test method used is in agreement with the procedure described in the EN 12975 standard as presented in the literature [2]. A very similar procedure to EN 12975 is described in ASHRAE [3]. The main difference between these is that initially, in the EN standard, the aperture of the collector should be shielded from the solar radiation by means of a solar-reflecting cover. Once the steady-state has been reached, the cover should be removed at the beginning of the measurement.

3.2. Steady-state collector characterization

The measurement procedure is based, as the time constant characterization, on the EN 12975-1 standard. According to this standard, the collector must be tested under clear sky conditions around solar noon. The performance of the collector thermal parameters can be calculated by curve fitting, using the least square method. More details about this procedure are given in Ref. [3]. The steady-state results are used as reference values for comparing with model results. The data set was measured during two stable days and led to the collection of 16 experimental points.

3.3. Dynamic collector characterization

The experiment, according to the dynamic model described in Section 2, was performed using a closed-loop collector. Basically, the test set-up has similar configuration to that of the steady-state [3]. In order to have a good comparison with the steady-state results, the dynamic measurements were taken always with the sun perpendicular to the collector. This condition is possible to be reached due to the short measuring time period of time measurements needed as well as the use of a solar tracking system. The data were taken for a fixed low mass flow rate in order to increase the heat transfer process due to the small surface area of the PV/T collector (Table 1). The same mass flow rate which was applied was kept constant during all the measurement tests.

All the instruments and sensors were connected to datalogger CR23X. The inlet and outlet fluid and ambient temperatures, wind speed and solar radiation data were measured using type-K thermocouples, a Vector A-100R cup anemometer and a Kipp & Zonen CMP 11 pyranometer, respectively. The mass flow rate of the working fluid was accurately regulated by using a precision peristaltic pump (Percom N-M) which pumped at a constant known flow rate of 3.17 g/s or 0.022 kg/m^{2}s. In order to achieve variations in inlet temperatures during the test, thermostatic immersion circulators capable of water heating with an accuracy of ±0.1 °C were used. Measurements were taken for several inlet and outlet fluid temperatures, ambient temperatures, wind speed and solar radiation values. The different input variables were measured every 1 s and their mean values were recorded every 10 s.

The tests were performed in a flat-plate solar collector at the Applied Energy Research Centre (CREA) at the University of Lleida (Spain) which is located in Lleida at latitude 41.36° N and longitude 0.37° E. The collected data were collected during outdoor tests in December 2010.

The measurement procedure for the dynamic characterization has been performed in a similar way to the collector time constant measurement. The major difference was that the solar radiation measurements, for this case, were performed under forced transient conditions using a shading screen. The screen reduces the intensity of the incoming solar radiation and thus the range of variation and the thermal capacitance effects are increased. This manipulation can be used for a short time period instead of the total day and is achieved by shielding the collector area for a specific time interval and then exposing it to the sun. At least three

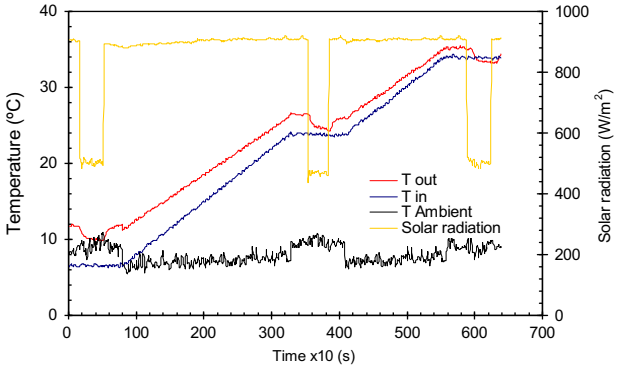

Fig. 3. Experimental measured data for the collector testing characterization under forced transients conditions.

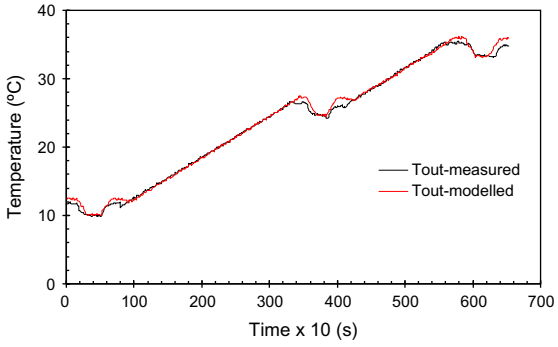

Fig. 4. Comparison of the outlet temperature between modelled and measured values.

different constant inlet temperatures are required to complete the measurement process. One test sequence of them should be conducted with the inlet fluid temperature close to the ambient temperature in order to get the accurate value of zero loss efficiency parameter. The other two sets should be performed close to the middle and the highest of the temperature operation, respectively. In addition, the inlet fluid temperature can vary between subsequent constant inlet temperature time periods, as shown in Fig. 3.

4. Results and discussion

4.1. Model calibration

A set of experimental data (Fig. 3) was used to calibrate through the optimization of model parameters. The calibration was applied to the outlet fluid temperature by using the linear least square method. In Fig. 3, a quite constant radiation when the collector is uncovered, can be seen. The ambient temperature was very stable, as the data were collected around at noon, achieving maximum variations of around 4 °C. For this specific data set, the outlet experimental temperature and the simulated one after the optimization involved in the calibration are illustrated in Fig. 4. From this figure, it can be seen that both sets of data are almost superposed, denoting a good behavior of the model.

The optimization function is that which minimizes the sum of squares of differences between the predicted and the measured values. The optimized parameters for minimizing the objective function are: $F'(\tau\alpha)$, $F'U_L$ and $M_e c_e$. These parameters are then considered as fixed and used for all the other simulations included the validation ones. A comparison of $F'(\tau\alpha)$ and $F'U_L$ with those obtained under steady-state conditions are presented in Table 2,

Table 2
Calibration results for the characteristic parameters of the model and comparison with those corresponding to the steady-state conditions.

	Steady-state		Dynamic-state piston flow concept	
Parameters	Value ± SE (95% CI)	*t*-Ratio value	Value ± SE (95% CI)	*t*-Ratio value
$F'(\tau\alpha)_{en}$ (–)	0.518 ± 0.008	64.7	0.498 ± 0.003	142.7
$F'U_L$ (W/(m^{2}K))	14.2 ± 0.4	39.4	14.26 ± 0.15	105.7
$M_e c_e/A_c$ (kJ/K)	–	–	12.9 ± 0.4	36.0

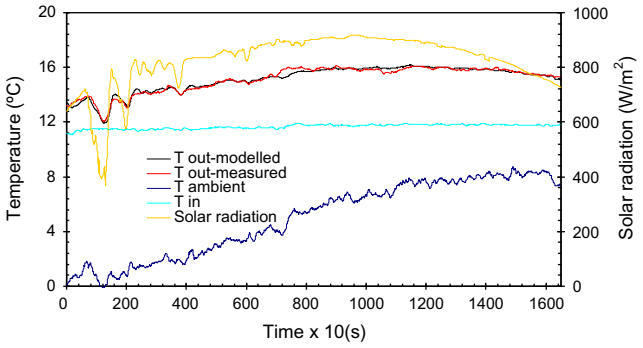

Fig. 5. Measured and modelled data used in the validation, under constant inlet temperature, corresponding to a time period of approximately 4 h (2.5 before and 1.5 after the solar noon).

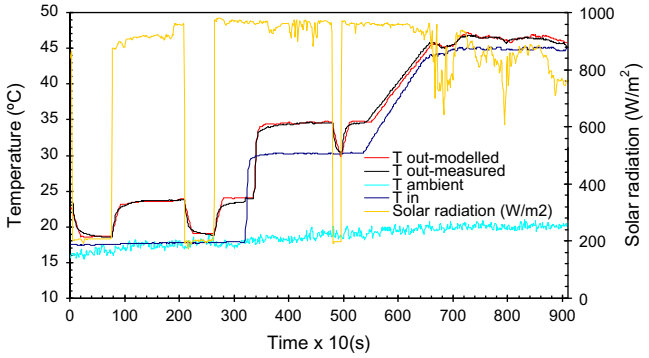

Fig. 6. Measured and modelled data used in the validation, under variable inlet temperature, by applying the forced transient conditions.

where can be noticed that the results of the dynamic-state are practically the same to those of the steady-state testing.

The modelling was applied to the data within an appropriate number of segments N corresponding with the interval time (Eq. (14)). The number of segments was found to be 14 (interval time 10 s), associated with the length of the time constant (90.2 s). As reported by [9] the interval time must be associated to the climatic data. From the analysis performed it can be concluded that it is necessary to relate the interval time with the time constant, instead of the weather data variations; this happens because the collector itself actuates as a filter for the climatic data with variability lower than the constant. The algebraic expression for the outlet temperature (Eq. (7)) depends directly on the integrated value of the T_a and G extended to an integration interval equal to the collector transport time.

The outlet fluid temperature based on the simple algebraic equation obtained from the model agrees reasonably with those of the measured values as shown in Fig. 4. This means that the appropriate number of segments used in the model gives satisfactory results in terms of the heat transport time. On the other hand, the effective heat capacity parameter ($M_e c_e$) for a given flow rate is well represented by the heat transport time of the collector as well as the specific heat fluid flow rate (Eq. (12)). Furthermore, the *t*-ratio analysis used for the evaluation in the linear regression process is also presented in Table 2. The *t*-ratio is defined as the parameter value divided by the standard deviation of this parameter obtained through regression. All the *t*-ratio values of the parameters should be greater than the critical value. In the conditions of the experiment, the critical *t*-ratio values were 1.9 for the steady-state and 1.5 for the dynamic-state, which was used as a reference.

The confidence interval (CI) in the statistical process has been selected to be 95%. It can be seen that all the *t*-ratio values obtained for the parameters of the dynamic model are well accepted in comparison to the critical ones. This means that the parameters in the regression equation are useful in predicting the assessed values of this model. The *t*-ratio values obtained for the dynamic parameters are much higher than those of the steady-state test. The difference is mainly due to the larger number of data available during dynamic-state measurements compared with the small number data of the steady-state test.

4.2. Validation of the model

Validation concerns the analysis and comparison of an experimental data set, different to the one used for the calibration, with the model results for the same initial conditions. A variable data range is used to confirm that the model matches the corresponding experimental values.

The collector outlet temperature, as it could be the power, is a very good parameter to compare the result of the model which simulates the collector. In terms of the other validation cases, the modelled data are included in the same graph with the experimental ones (Figs. 5 and 6). Fig. 5 illustrates a constant inlet fluid temperature for a partly cloudy day before the solar noon and for a mostly clear day after solar noon (the data presented refer to approximately two hours before and after the noon).

In Fig. 5, the inlet temperature was kept constant for all the experiments by using a thermostatic bath. During the day of the data collection, in the beginning, the weather was quite cloudy and very cold (registered temperatures around 0 °C). After the noon the sky started to clear and the temperature rose accordingly. Under variable conditions, the simulation model represents perfectly the tendency of the outlet temperature at each time instant.

Furthermore, in Fig. 6 the final of the validation scenarios is illustrated. This case regards a combination of variable inlet temperatures under forced, transient conditions and partly cloudy day. Under these variable conditions, the response of the model is satisfactory, showing a coefficient of determination of 0.999 with the outlet temperature (see Fig. 8).

For the model validation process (Figs. 5 and 6) the predicted values closely match the measured data. Even when the inlet temperature was gradually increased the model gives reasonably good results; thus, allows a flexibility which is a great advantage. In this way restrictive requirements in the constant inlet fluid temperature during measurements necessary in the other methodologies discussed in Section 1, are avoided. The good behavior of the model

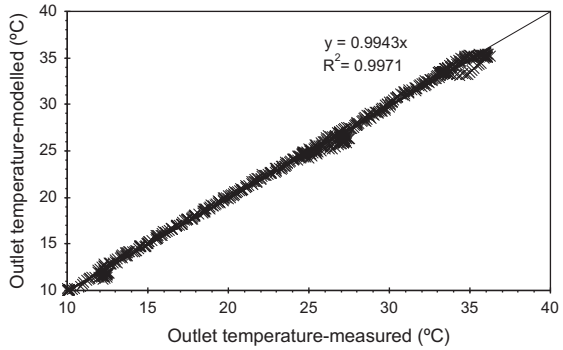

Fig. 7. Correlation between measured and modelled outlet temperatures for the collector calibration process, according to Fig. 4.

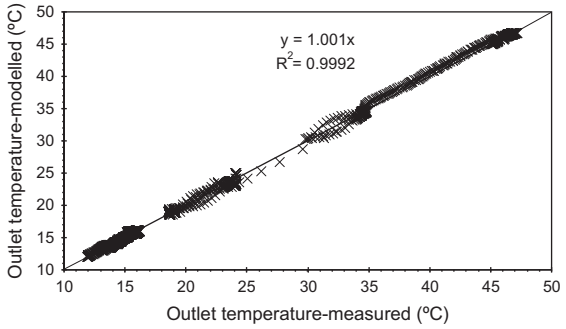

Fig. 8. Comparison between the simulated and measured outlet temperature values for model validation; regards the data shown in Figs. 5 and 6.

is clearly stated in the calculation of the standard error in terms of the prediction between simulated and measured outlet temperature values. Regarding the scenarios depicted in Figs. 5 and 6, the errors were calculated to be 0.22 °C and 0.37 °C, respectively. The first error value is almost half of the second. This difference can be attributed to the forced transient conditions, which result in abrupt changes and thus difficulties arise in the dynamic simulation. This inaccuracy can be seen in a small number of scatter points which appear in the simulated curves (forced, transient conditions). Some large discrepancies are related to the differences in the outlet temperature (approximately 1 °C).

Simulated and experimental results can easily be compared by representing both at the same graph and observing discrepancies. If the simulation values fit perfectly the experimental ones, the result should be the line 1:1 (slope equal to 1 and y-interception equal to 0). In Figs. 7 and 8 the comparison between simulated and experimental data (Fig. 4: calibration process; Fig. 6: validation process) is illustrated. It can be noted that in both cases the coefficient of determination is greater than 0.997 and the discrepancy on the slope with respect to the theoretical value (1) is less than 0.6%. The analysis of the t-ratio value of the independent term is in both cases lower than the critical t-ratio. This means that the above mentioned coefficient has no significance or, in other words, the null value hypothesis of this term is not rejected and then it should be set equal to 0.

Due to the linear response and good correlation with the experimental data, for both the calibration and validation process, the model can be used to predict the outlet temperature and thermal production of the collector using the appropriate climatic data. This characteristic is the main advantage of the proposed methodology in comparison with the norm EN 12975. To predict using the EN standard model it is necessary to make a recursive process to interpolate the average fluid temperature involved in the derivative term.

5. Conclusions

A new transient model for the thermal characterization of collectors using the piston flow concept was developed. The model was calibrated and validated with results obtained from experimental data. It includes an algebraic equation for the calculation of the water outlet temperature. By using this simple algebraic equation, the new method could easily be applied to any available spreadsheet program. It does not require a special program with ODE system solver as proposed by DSC model.

The algebraic expression for the water outlet temperature (Eq. (7)), depends directly on the integrated values of T_0, T_a and G extended for interval of integration equal to the heat transport time of the collector. The characteristic parameters of the model are the $F'(\tau\alpha)$ and $F'U_L$ and did show agreement with the results obtained from standard steady-state measurements. Furthermore, the effective thermal capacity parameter ($M_e c_e$) was taken into account by the heat transport time of the collector and the characterization process was related with at least three different levels of inlet temperatures as well as a forced radiation process for each level. The correlation between experimental and simulated data was shown to be significant with the 1:1 line. In addition, the analysis of the t-ratio value of the independent term was for both cases lower than the critical t-ratio.

The model requirement is: $N\Delta t = (1 - e^{-1})^{-1}\tau_c$. This means that the time interval used to collect the experimental data should be at least an order-of-magnitude lower than the time constant. This assures that the simulated system will achieve exactly the same time constant than the experimental one.

The calibration process can be performed using either constant or variable inlet temperatures, achieving in both cases equivalent results. Once calibrated, the model can be used to accurately predict the outlet temperature and thermal production of the collector for a specific set of climatic data from variable radiation and temperatures. This characteristic is the main advantage of the proposed methodology in comparison with the norm EN 12975.

Acknowledgements

The authors acknowledge the financial support from the General Directorate of Higher Education (GDHE) of Indonesia and the Ministry of Science and Technology, Spain (MCYT)-(ENE 2010-18357). Furthermore, the authors wish to acknowledge Dr. Josep Conde for his fruitful comments and suggestions concerning the statistical analysis.

References

[1] ISO Standard 9806-1. Thermal performance of glazed liquid heating collectors; 1994.
[2] Eropean Standard EN 12975:2006, CEN, European Committee for Standardisation; 2006.
[3] ANSI/ASHRAE Standard 93-2003. Methods of Testing to Determine Thermal Performance of Solar Collectors; 2006.
[4] Perers B. Dynamic methods for solar collector array testing and evaluation with standard database and simulation programs. Solar Energy 1993;50(6):517–26.
[5] Isakson P. Solar collector model for testing and simulation, Doctoral Thesis, Royal Institute of Technology, Sweden; 1995.
[6] Muschaweck J, Spirkl W. Dynamic solar collector performance testing. Solar Energy Mater Solar Cell 1993;30:95–105.
[7] Nayak JK, Amer EH, Deshpande SM. Comparison of three transient methods for testing solar flat-plate collectors. Energy Convers Manage 2000;41:677–700.
[8] Scnieders J. Comparison of the energy yield predictions of stationary and dynamic solar collector models and the model's accuracy in the description of a vacuum tube collector. Solar Energy 1997;61:179–90.
[9] Taherian H, Rezania A, Sadeghi S, Ganji DD. Experimental validation of dynamic simulation of the flat plate collector in a closed thermosyphon solar water heater. Energy Convers Manage 2011;52:301–7.